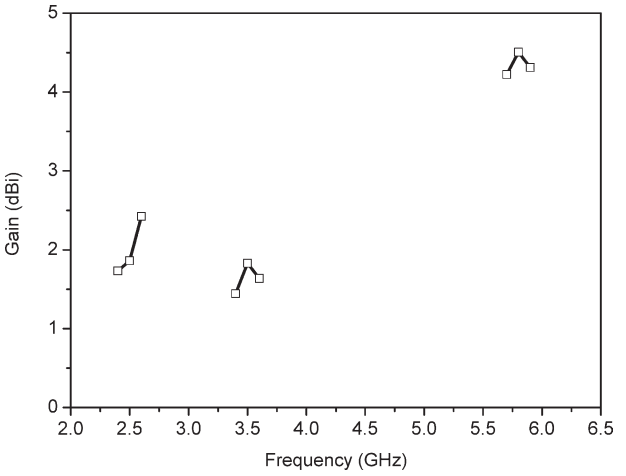

Figure 8 Peak gains of the proposed antenna

4. CONCLUSIONS

In this article, a novel compact microstrip-fed monopole antenna with two strips (a horizontal strip and a spiral strip) for triple-band operation has been designed and successfully implemented, with experimental and numerical results. The proposed antenna can provide sufficient impedance bandwidth and suitable radiation patterns for 2.4/5.8 GHz WLAN and 3.5 GHz WiMAX systems. Omnidirectional radiation performance and sufficient gain can also be obtained. The measured results of the constructed prototype show good agreement with the simulated ones, and larger effects of varying some important parameters on the antenna resonant frequencies have also been examined. The antenna has a small size of dimensions 12×32 mm^2 and is a good candidate for WLAN and WiMAX applications.

REFERENCES

1. Y.F. Lin, H.D. Chen, and H.M. Chen, A dual-band printed L-shaped monopole for WLAN applications, Microwave Opt Technol Lett 37 (2003), 214–216.
2. Y.L. Kuo and K.L. Wong, Printed double-T monopole antenna for 2.4/5.2 GHz dual-band WLAN operations, IEEE Trans Antennas Propag 51 (2003), 2187–2192.
3. G.L. Xin and J.P. Xu, Wideband miniature G-shaped antenna for dual-band WLAN applications, Electron Lett 24 (2007), 1330–1332.
4. S.H. Yeh and K.L. Wong, Dual-band F-shaped monopole antenna for 2.4/5.2 GHz WLAN application, In Proceedings IEEE Antennas Propagation Symposium, San Antonio, TX, 2002, pp. 72–75.
5. Y. Song, Y.C. Jiao, H. Zhao, Z. Zhang, Z.B. Weng, and F.S. Zhang, Compact printed monopole antenna for multiband applications, Microwave Opt Technol Lett 50 (2008), 365–367.
6. W.-C. Liu, C.-M. Wu, and Y. Dai, Design of triple-frequency microstrip-fed monopole antenna using defected ground structure, IEEE Trans Antennas Propag 59 (2011), 2457–2463.
7. W.-S. Chen and K.-Y. Ku, Band-rejected design of the printed open slot antenna for WLAN/WiMAX operation, IEEE Trans Antennas Propag 56 (2008), 1163–1169.
8. Y.P. Chen, T.S. Hong, W.S. Chen, and H.H. Chen, Dual wideband printed monopole antenna for WLAN/WiMAX applications, IEEE Antennas Wirel Propag Lett 6 (2007), 149–151.
9. K.G. Thomas and M. Sreenivasan, A novel triple band printed antenna for WLAN/WiMAX applications, Microwave Opt Technol Lett 51 (2009), 2481–2485.

IN SITU CHARACTERIZATION OF PIN DIODE WAVEFORMS USING ELECTRO-OPTIC SAMPLING

Evelyn Benabe,[1] Matthew H. Crites,[2] John F. Whitaker,[2] and Thomas M. Weller[1]
[1] University of South Florida, Tampa, FL 33620; Corresponding author: weller@usf.edu
[2] University of Michigan, Ann Arbor, MI 48109-2099

Received 14 February 2012

ABSTRACT: *In situ measurements of nonlinear waveforms produced by a PIN diode under large-signal excitation have been performed using ultrafast electro-optic (EO) sampling. The waveforms were sampled using an EO probe positioned immediately after the diode. These data validate a nonlinear model and improve representation of the waveform across the circuit.* © 2012 Wiley Periodicals, Inc. Microwave Opt Technol Lett 54:2653–2656, 2012; View this article online at wileyonlinelibrary.com. DOI 10.1002/mop.27119

Key words: *electro-optic sampling; nonlinear; PIN diode; time-domain*

1. INTRODUCTION

Time-domain electro-optic (EO) characterization of periodic electrical waveforms, which uses ultrafast laser pulses as delta-function-like sampling gates within optical sensor crystals placed at key signal locations, has been practiced for more than 20 years [1, 2]. Unlike conventional EO sampling, the system in this work used a single beam of optical probe pulses synchronized with the RF input to the device under test (DUT), and an optical-time-delay translation stage was used to sweep the sampling-gate pulses through the DUT output repetitive waveforms. An ultrabroad-bandwidth EO probe, located immediately adjacent to the output of the device, was used to obtain in situ measurements.

Of particular interest in this work was the characterization of a limiter PIN diode driven in the large-signal regime. An important parameter describing the performance of a PIN diode is the recovery time, both forward and reverse, which depends on the dynamic bias condition of the device. This bias dependence leads to relatively complex behavior in terms of signal distortion at high RF drive levels and consequently poses challenges in developing scalable large-signal equivalent circuit models. It is typical that such models use a transit time parameter, associated with a diffusion capacitance, to capture this device-speed-related characteristic.

Herein it is demonstrated that the ability to accurately measure the waveform in situ, immediately at the device output and free of dispersion from assorted interconnects, facilitates the observation of sub-ns features in the waveform. Subsequently, it is shown that the EO data can be used to validate the nonlinear PIN diode model, and in particular the transit time value. The morphology of the dynamic voltage across the diode is strongly dependent on the transit time under nonlinear operating conditions, and thus the EO data provide a means of validating nonlinear, frequency- and time-domain simulations.

2. FIXTURE DESIGN AND PIN DIODE MODEL

The EO measurements in this study were performed on a packaged PIN diode mounted in a two-port microstrip test fixture with high-frequency coaxial connectors at each end. The device is a Micrometrics MLP7110-19-1 PIN diode. Per vendor specifications, the part has a minimum breakdown voltage of 45 V and

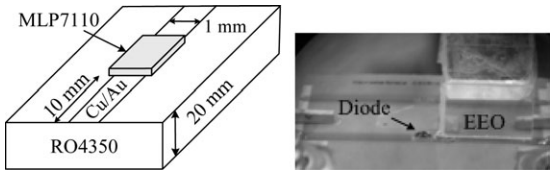

Figure 1 (Left) PCB fixture used for EO characterization of PIN diode. (Right) Photograph of the EO probe positioned above the output microstrip. The laser beam was focused into the EO crystal 1 mm above the microstrip

a series resistance of 1.5 Ω at 10 mA (∼0.85 V). It is rated to operate from 100 MHz to beyond 20 GHz. The test fixture, shown in Figure 1, consisted of 50 Ω microstrip transmission lines printed on a 20-mil-thick RO4350 Rogers Corp. substrate.

A simplified nonlinear model for the PIN diode, based on Ref. 3, is given in Figure 2. R_s is a parasitic resistance and R_v represents the bias-dependent I-region resistance of the device; in strong reverse bias $R_v \rightarrow \infty$, and the parallel combination of resistors reaches a limit of R_{max}. C_j is a bias-dependent junction capacitance, whereas C_d is a capacitance linked to the finite transit time through the I-region. In the model, C_d is proportional to a transit time parameter and the diode current, I_d. In practice, PIN diodes are characterized by forward and reverse switching speeds that depend upon the carrier lifetime, I-region width, and the operating point (bias) conditions. In the model used herein, as in most models, the switching speeds cannot be explicitly defined because of their dependence on the quiescent (initial) operating point and the operating point to which the diode is switched. Thus in this work, the switching speed is adjusted to best match the measurement (EO) data, and the parameter that is used to emulate switching speed is the transit time.

3. EO MEASUREMENT SETUP

Time-domain EO sampling commonly uses repetitive optical pulses derived from a mode-locked laser as sampling gates, using synchronization of these pulses to the periodic voltage output of a signal generator and some variable delay to sample the electrical response of a DUT. Time-resolved transients, as well as the amplitude and phase of sinusoidal signals, have been measured using different versions of these methods [4, 5]. In all cases, the RF electric field fringing around a conductor changes the refractive index of the EO sensor medium and slightly modulates the light traveling through the sensor via the Pockels effect.

As depicted in Figure 3, an optical embodiment was devised to characterize the large-signal response of the PIN-diode DUT. A 10-MHz reference signal, derived from a laser-repetition-rate stabilization circuit, was used to phase-lock the 80 MHz, 100-fs-duration pulsed output of a titanium-doped-sapphire solid-state laser with the output of the RF signal source for the DUT.

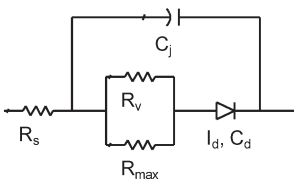

Figure 2 PIN diode equivalent circuit model (after Ref. 3). R_s and R_{max} are constant values; all other parameters are nonlinear

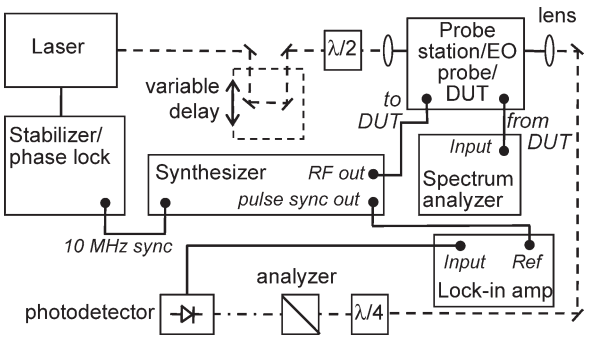

Figure 3 EO sampling experimental configuration: red (dashed) line is optical beam path; black (solid) lines are electrical connections. $\lambda/2$ and $\lambda/4$ are half and quarter-wave retarders, respectively

Simultaneously, a moving-mirror variable delay was used to adjust the synchronization between the ultrafast laser sampling-gate pulses and the DUT waveforms.

To measure the voltage transients, the polarization of the laser was initially set by a half-wave plate, and the beam was focused to a ∼ 50-μm-diameter spot inside a 600-μm-thick lithium tantalate ($LiTaO_3$) dielectric probe crystal. The optic axis of the probe was oriented normal to the plane of the microstrip, and the laser traveled parallel to the microstrip plane and normal to the electrical propagation direction so that the normal electric field above the strip was sensed. The resulting polarization modulation on the laser pulses was converted into an optical-intensity modulation using a quarter-wave plate, a polarization analyzer, and a photodetector.

With the RF source signal to the DUT synchronized to the same 10-MHz signal that stabilizes the laser pulsing rate, the laser sampling pulses would each arrive in the sampling crystal at the same point in the cycle of the periodic electrical waveforms, given that the synthesizer was set to an integer multiple of 80 MHz. The delay of the sequential sampling-gate pulses—which were effectively delta functions given the laser pulse width of 100 fs and the ultrafast response time of $LiTaO_3$—was achieved by changing the optical path length with a motorized linear translation stage and a retroreflector mirror.

The optical-intensity-modulation information obtained at each optical-delay position was placed within a narrow measurement bandwidth using an additional, 3.33-MHz square-wave pulse modulation on the DUT input (and thus also on the periodic RF waveform appearing at the output); this effectively turned the DUT input RF on and off at a frequency that was also available for use as a reference for a lock-in amplifier readout instrument (see Fig. 3).

The details of the RF signal path used in the experimental setup are given in Figure 4. The RF source in this figure (corresponding to the ''RF out'' location in Fig. 3) drives an amplifier that is used to achieve the desired power at the input of the

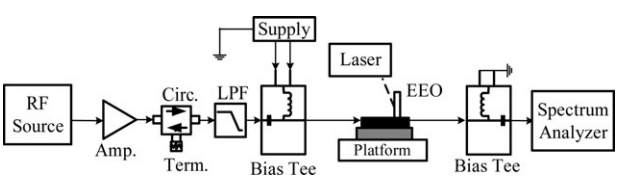

Figure 4 Microwave setup used to provide the modulated carrier to the DUT

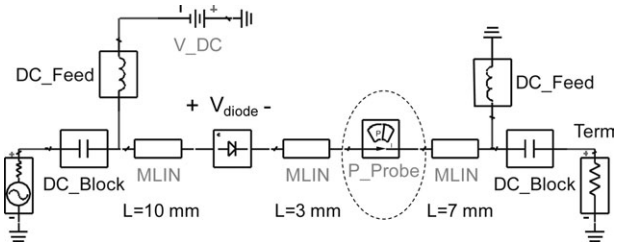

Figure 5 Schematic representation of the test configuration

DUT. The low pass filter ensures that the nonlinear behavior measured is that of the DUT alone.

4. TIME-DOMAIN WAVEFORM ANALYSIS

In this section, measured waveforms using the EO setup are compared against data obtained from transient simulations. The simulations were performed using Agilent Technologies advanced design system (ADS) and the schematic shown in Figure 5, which includes the nonlinear PIN diode model. The EO probe location is represented by the *P_Probe* symbol in the

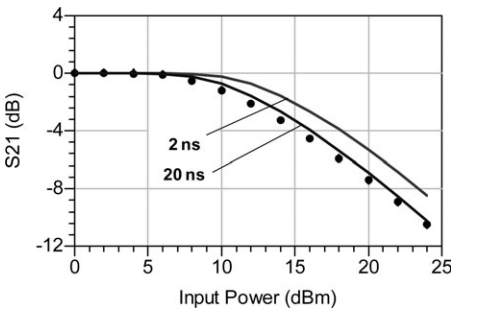

Figure 7 Large-signal S_{21} with the PIN diode in a shunt two-port test fixture: measured data (markers) and simulated results using 2 and 20 ns transit time settings

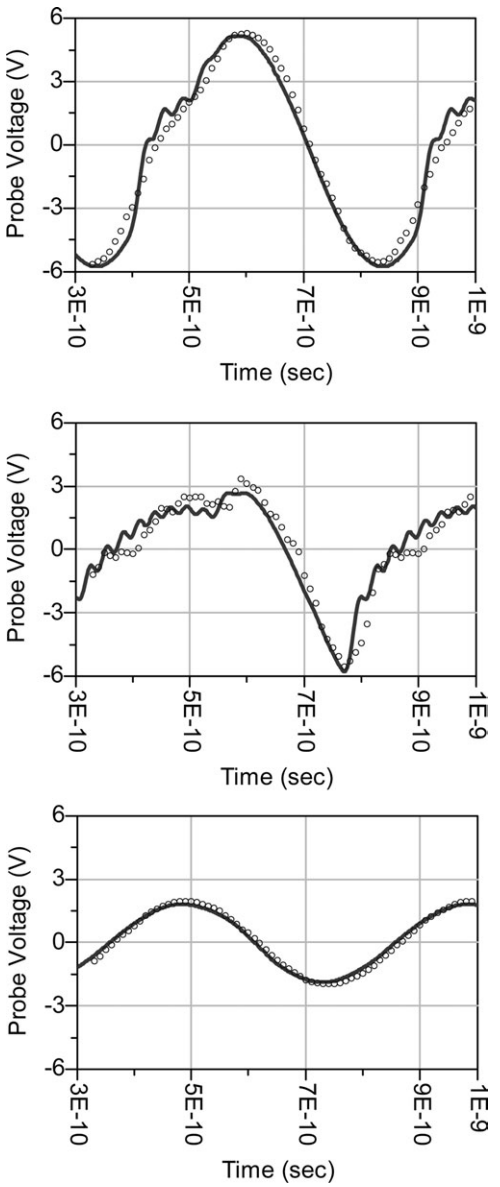

Figure 6 Probe voltage for 2 GHz drive level of 25 dBm at (clock-wise from top left) 0, −5, and −12 V DC bias (markers: EO-measurement data)

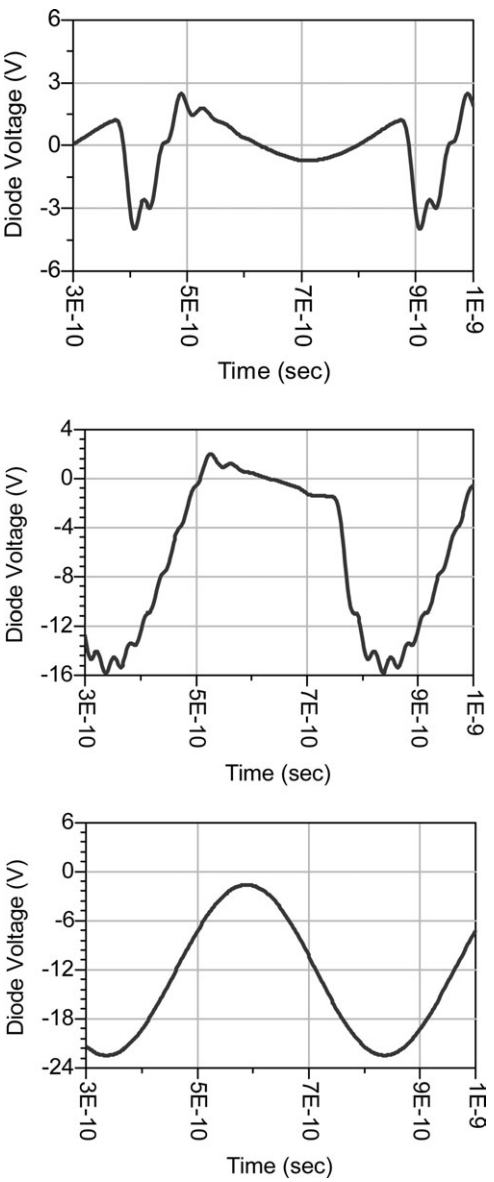

Figure 8 Diode voltage (V_{diode}) for 2 GHz drive level of 25 dBm at (clock-wise from top left) 0, −5, and −12 V DC bias

schematic, and the voltage measured at this point is referred to as the probe voltage. A scale factor of 0.07 V/μV was applied to all measurement data to correct for the difference between the probe voltage on the transmission line (ADS data) and the lock-in voltage corresponding to the field sensed above the line by the EO probe.

The data in Figure 6 correspond to tests using 2 GHz, 25 dBm RF signals with varying DC bias across the diode. These results show the progression from a distorted (harmonic-rich) waveform to a pure sinusoid as the bias increases from 0 to -12 V. These simulations were performed using a PIN diode transit time setting of 20 ns. The simulations also confirm that the waveform remains linear for larger reverse-bias levels, which could be important for applications such as PIN diode attenuators.

Large-signal S_{21} (power compression) measurements further validate the accuracy of the nonlinear model. In Figure 7, simulated and measurement data are plotted versus input power with the PIN diode mounted in a two-port shunt test fixture without DC bias. The simulations were performed using transit time settings in the model of 2 and 20 ns, to illustrate the dependence on this parameter.

Having demonstrated excellent agreement with the time- and frequency-domain measurements, the nonlinear model can be used to predict node voltages within the circuit with a high degree of confidence. Of particular interest is the voltage across the PIN diode (V_{diode} in Fig. 5). In Figure 8, this voltage is shown for the three conditions addressed in Figure 6, illustrating the magnitude and duration of forward bias in each case.

5. CONCLUSIONS

Internal-node EO sampling provides a unique capability for in situ examination of waveforms, including locations of harmonic generation in a microwave circuit. This information has been shown to be useful in validating nonlinear models. As a result, more accurate predictions of transient waveforms and internal voltages are possible.

ACKNOWLEDGMENT

This work was supported in part by the National Science Foundation (Grant #ECS-0601536 and #ECS-0901779).

REFERENCES

1. J.A. Valdmanis, 1 THz-bandwidth prober for high speed devices and integrated circuits, Electron Lett 23 (1987), 1308–1310.
2. K.J. Weingarten, M.J.W. Rodwell, and D.M. Bloom, Picosecond optical sampling of GaAs integrated circuits, IEEE J Quantum Electron 24 (1988), 198–220.
3. S. Iordanescu, G. Simion, C. Anton, and A. Muller, Broadband microwave PIN diode attenuators, In: Semiconductor Conference, 1998. CAS '98 Proceedings. 1998 International, vol. 2, 6–10 October 1998, pp. 601–604.
4. T. Löffler, T. Pfeiffer, H.G. Roskos, H. Kurz, and D.W. van der Weide, Stable optoelectronic detection of free-running microwave signals with 150-GHz bandwidth, Microelectron Eng 31 (1996), 397–408.
5. J.F. Whitaker and K. Yang, Electro-optic sampling and field mapping, In: M.E. Fermann, A. Galvanauskas, and G. Sucha (Eds.), Ultrafast lasers, technology and applications, Marcel Dekker AG, New York, 2000, pp. 473–519.

A NEW DESIGN OF SMALL SQUARE MONOPOLE ANTENNA WITH ENHANCED BANDWIDTH BY USING CROSS-SHAPED SLOT AND CONDUCTOR-BACKED PLANE

Behrang Hadian Siahkal-Mahalle,[1] Nasser Ojaroudi,[2] and Mohammad Ojaroudi[3]

[1] Department of Electrical Engineering, Aeronautical University of Science and Technology, Tehran, Iran

[2] Department of Electrical Engineering, Ardabil Branch, Islamic Azad University, Ardabil, Iran

[3] Young Research Club, Ardabil Branch, Islamic Azad University, Ardabil, Iran; Corresponding author: m.ojaroudi@iauardabil.ac.ir

Received 15 February 2012

ABSTRACT: *We present a novel printed monopole antenna for ultrawideband applications. The proposed antenna consists of a square radiating patch and a ground plane with cross-shaped slot and conductor-backed plane, which provides a wide usable fractional bandwidth of more than 130% (3.06–12.87 GHz). By cutting a modified cross-shaped slot with variable dimensions on the ground plane and also by inserting cross-shaped conductor-backed plane, additional resonances are excited and hence much wider impedance bandwidth can be produced, especially at the higher band. The designed antenna has a small size of 12 × 18 mm^2. Simulated and experimental results obtained for this antenna show that it exhibits good radiation behavior within the UWB frequency range.* © 2012 Wiley Periodicals, Inc. Microwave Opt Technol Lett 54:2656–2659, 2012; View this article online at wileyonlinelibrary.com. DOI 10.1002/mop.27138

Key words: *square monopole antenna; cross-shaped slot; conductor-backed plane; ultrawideband communication systems*

1. INTRODUCTION

In UWB communication systems, one of key issues is the design of a compact antenna while providing wideband characteristic over the whole operating band. Consequently, number of monopoles with different geometries have been experimentally characterized [1, 2]. Moreover, other strategies to improve the impedance bandwidth have been investigated [3, 4].

This letter focuses on a square monopole antenna for UWB applications, which achieves a fractional bandwidth of more than 130%. In this structure by cutting a modified cross-shaped slot and conductor backed plane with variable dimensions on the ground plane, additional resonances (third and fourth resonances) are excited. By obtaining the third and fourth resonances, the usable upper frequency of the monopole is extended from 10.3 to 12.87 GHz. The designed antenna has a small size of 12 × 18 mm^2, and the impedance bandwidth of the designed antenna is higher than the UWB antennas reported recently [1–4]. As a result, unlike other antennas reported in the literature to date [1–4], the proposed antenna displays a good omnidirectional with low cross-polarization level radiation pattern even at higher frequencies.

2. ANTENNA DESIGN

The proposed square monopole antenna is shown in Figure 1, which is printed on a FR4 substrate of thickness 1.6 mm, permittivity 4.4. Regarding defected ground structures, the creating slots in the ground plane provide an additional current path. Moreover, this structure changes the inductance and capacitance of the input impedance, which in turn leads to change the bandwidth [3, 4]. Therefore, by cutting a cross-shaped slot at the ground plane, much enhanced impedance bandwidth may be